A New Water-Soluble Phosphine Derived from 1,3,5-Triaza-7-phosphaadamantane (PTA),† 3,7-Diacetyl-1,3,7-triaza-5-phosphabicyclo[3.3.1]nonane. Structural, Bonding, and Solubility Properties

Donald J. Darensbourg,* Cesar G. Ortiz, and Justin W. Kamplain‡

Department of Chemistry, Texas A&M University, College Station, Texas 77843

Received November 18, 2003

The phosphine 3,7-diacetyl-1,3,7-triaza-5-phosphabicyclo[3.3.1]nonane, which we will condense to DAPTA, and its oxide have been fully characterized both in solution and in the solid state. These compounds were prepared by acylation of 1,3,5-triaza-7-phosphaadamantane (PTA) and its oxide with acetic anhydride. The nonionic compounds were found to be soluble in most common organic solvents, in addition to possessing extremely large molar solubilities in water. Indeed, the molar solubility of DAPTA was shown to be 7.4 M, which is 4 time more soluble than the commonly utilized water-soluble phosphine, triply *meta*-sulfonated triphenylphosphine (TPPTS). In the case of DAPTA this enhanced water solubility is attributed to a strong interaction of water with the amide nitrogen−CO bond dipole as revealed by a large red shift of the $\nu_{C=O}$ vibration on going from a weakly interacting solvent such as CH_2Cl_2 to water. This latter observation is supported by the short average amide nitrogen−carbonyl carbon bond distance of 1.375 Å as determined via X-ray crystallography, indicative of a strong Coulombic interaction between the nitrogen and carbon atoms. To assess the metal to phosphorus binding characteristics of DAPTA, several group 10 and group 6 complexes were prepared and their M−P bond distances were shown to be quite similar with those of their PTA analogues. For examples, the W−P bond distance in $W(CO)_5$DAPTA of 2.492(3) Å is comparable to that previously reported for $W(CO)_5$PTA of 2.4976(15) Å and slighter shorter than that found in $W(CO)_5PMe_3$ (2.516(2) Å). Accordingly, the PTA ligand has generally been characterized as possessing donor properties similar to that of PMe_3. Consistent with these bonding parameters determined in the solid state, all three tungsten pentacarbonyl complexes have nearly identical ν(CO) frequencies in solution.

Introduction

Aqueous organometallic chemistry has received much attention in recent years due to the many advantages an aqueous medium presents to stoichiometric and catalytic reactions.[1] Water's copious and nontoxic nature, along with its distinct physical properties, makes it an ideal solvent for numerous processes from an industrial point of view. With regard to its physical properties, its high heat capacity enables it to effectively distribute heat from exothermic reactions, and its immiscibility with many organic compounds allows it to serve as part of a biphasic system where products can be easily separated from water-soluble catalysts by a simple extraction process. The latter procedure is the foundation of the Ruhrchemie−Rhône Poulenc hydroformylation process of lower molecular weight olefins,

Chart 1

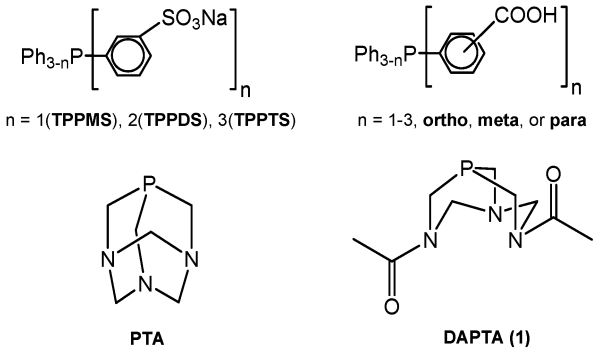

in which the triply *meta*-sulfonated triphenyl phosphine ligand, TPPTS, is used with rhodium as the active metal center.[1,2] This and other tertiary water-soluble phosphines (WSP) have been the most widely used class of water-soluble ligands in aqueous catalysis due to their neutral donating ability, which can effectively stabilize the metal center throughout the catalytic cycles (Chart 1). Furthermore, these phosphines can participate in the reduction of the metal center in such processes as carbon−carbon bond formation reactions, where group

† The IUPAC name for PTA is 1,3,5-triaza-7-phosphatricyclo[3.3.1.1^{3,7}]-decane.

* Corresponding author. Fax: (979)845-0158. E-mail: djdarens@mail.chem.tamu.edu.

‡ NSF-REU participant from Oklahoma Christian University.

(1) For extensive reviews on aqueous catalysis, see: (a) Joó, F. *Aqueous Organometallic Catalysis*; Kluwer: Dordrecht, 2001. (b) Cornils, B., Herrmann, W. A., Eds. *Aqueous-Phase Organometallic Catalysis. Concepts and Applications*; Wiley-VCH: Weinheim, 1998. (c) Horváth, I. T., Joó, F., Eds. *Aqueous Organometallic Chemistry and Catalysis*; NATO ASI 3/5; Kluwer: Dordrecht, 1995. (d) Sinou, D. *Top. Curr. Chem.* **1999**, *206*, 41.

(2) Cornils, B. *Org. Process Res. Dev.* **1998**, *2*, 121.

10.1021/om0343059 CCC: $27.50
Publication on Web 03/09/2004

10 metals, M^{2+}, are reduced to the active M^0 species. Apart from TPPTS, a variety of WSPs have appeared through the years, and their catalytic potential has been investigated. Of main importance to our work is the water-soluble and air-stable 1,3,5-triaza-7-phosphaadamantane (PTA) ligand, which owes its water solubility to hydrogen bonding of the nitrogen atoms to water (Chart 1).[3] Due to its small cone angle (102°) and excellent donating ability (comparable to PMe_3), it has received much attention as a potential ligand for catalytic reactions such as in the monophasic[4] and biphasic[5] hydrogenation of alkenes and aldehydes.

In addition, various other derivatives of PTA have also been synthesized but remain relatively unexplored. For example, the sulfone derivative of PTA, 2-thia-1,3,5-triaza-7-phosphaadamantane-2,2-dioxide ($PASO_2$), was previously prepared by Daigle,[6] and its binding to group 6 metals[7] was illustrated in our laboratories. However, to our surprise, the $PASO_2$ derivative possesses very limited water solubility. Shortly after Daigle's initial synthesis of PTA, a series of reactions of PTA similar to those observed for its hexamethylenetetramine analogue were carried out by Siele. These included nitration,[8] nitrosation,[9] and acetylation.[10] At that time, it was noted that PTA reacts with acetic anhydride to provide the acetylated product 3,7-diacetyl-1,3,7-triaza-5-phosphabicyclo[3.3.1]nonane (**1**).[11] Nevertheless, no other studies of this phosphine, which we will call DAPTA, have been reported. Due to the need for a larger variety of water-soluble phosphines to serve as ligands to low-valent metal complexes rendering them soluble in water, we have chosen to investigate DAPTA for this purpose. Herein, we report the complete characterization of **1** and its corresponding oxide (**2**). In addition, several metal complexes were prepared and characterized in solution by IR/NMR spectroscopy, and in the solid state via X-ray crystallography, to assess the nature of the metal−phosphorus bond. The water solubility of **1** was measured and compared with other commonly utilized water-soluble phosphines, including its PTA analogue.

Experimental Section

Materials and Methods. Unless otherwise indicated, all reactions were carried out under an inert argon atmosphere using standard Schlenk and drybox techniques. Prior to their use, all organic solvents were distilled from sodium benzophenone ketyl. In the preparation of **1** and **2**, deionized water was used. $Cr(CO)_6$ and $W(CO)_6$ precursors were purchased from Aldrich Chemical Co., with the latter being sublimed prior to use. $Ni(COD)_2$ was purchased from Strem Chemical Co. and used without further purification. PTA and its oxide were prepared following the literature method.[3] Although the preparations of **1** and **2** have been previously described by Siele, the syntheses are included herein for completeness purposes.[11] The salicylaldimine used in the preparation of **4** was prepared according to the literature procedure.[12]

X-ray data were collected on a Bruker CCD diffractometer and covered more than a hemisphere of reciprocal space by a combination of three sets of exposures; each exposure set had a different φ angle for the crystal orientation, and each exposure covered 0.3° in ω. The structures were solved by direct methods. The absolute configuration of compound **1**, determined in the noncentrosymmetric space group $P2(1)$, could not be accurately assessed. ^1H, ^{13}C, and ^{31}P NMR data were obtained using a Varian Unity+ 300 MHz NMR instrument. ^1H and ^{13}C chemical shifts were referenced according to the deuterated solvent used. The ^{31}P chemical shifts were referenced using an external 85% H_3PO_4 sample. Elemental analyses were conducted by Canadian Microanalytical Inc.

Preparation of 3,7-Diacetyl-1,3,7-triaza-5-phosphabicyclo-[3.3.1]nonane (DAPTA) (1).[11] In a 250 mL round-bottom flask equipped with a dropping funnel, PTA (6.25 g, 39.6 mmol) was dissolved in 80 mL of water. To this solution, maintained at 0 °C, was added dropwise acetic anhydride (12.1 g, 119 mmol) with stirring over a period of 20 min. The solution was allowed to stand for 30 min, and the solvent was removed under vacuum, leaving behind a white solid. The product was purified by recrystallization from acetone and obtained in 47% yield. ^1H NMR (300 MHz, $CDCl_3$, δ): 1.96 (s, 6H, C(O)CH_3), 4.12 (d, $^4J_{PC}$ = 9.3 Hz, 4H, NCH_2N), 4.67 (d, $^2J_{PC}$ = 13.2 Hz, 2H, PCH_2N), 4.85 (d, $^2J_{PC}$ = 13.2 Hz, 2H, PCH_2N), 5.63 (d, $^2J_{PC}$ = 13.8 Hz, 2H, PCH_2N). ^{13}C NMR (75 MHz, $CDCl_3$, δ): 20.9 (C(O)*C*), 62.03 (N−C−N), 67.0 (P−C−N), 70.1 (P−C−N), 169.0 (C(O)). ^{31}P (121 MHz, $CDCl_3$, δ): −78.5. IR ($\nu_{C=O}$): 1642 cm^{-1} (CH_2Cl_2), and 1608 cm^{-1} (H_2O).

Preparation of 3,7-Diacetyl-1,3,7-triaza-5-phosphabicyclo[3.3.1]nonane 5-Oxide (2).[11] The preparation of **2** was achieved by the acylation of PTA oxide using a synthetic protocol analogous with that employed for the synthesis of **1**, in a 41% yield. Similar to **1**, the ligand readily dissolves in water and polar organic media such as methylene chloride and THF. ^1H NMR (300 MHz, $CDCl_3$, δ): 2.11 (s, 6H, C(O)CH_3), 3.27 (m, $^2J_{HH}$ = 16.2 Hz, $^4J_{PH}$ = 6.60 Hz, J_{HH} = 3.22 Hz, 1H), 3.74 (d, $^2J_{HH}$ = 7.20 Hz, 2H), 3.81 (dd, J_{PH} = 7.50 Hz, J_{HH} = 3.00 Hz, 1H), 3.87 (d, $^2J_{HH}$ = 14.4 Hz, 1H), 4.40 (t, $^2J_{HH}$ = 14.4 Hz, 1H), 4.87 (d, $^2J_{HH}$ = 14.1 Hz, 1H), 5.50 (t, $^2J_{HH}$ = 16.2 Hz, 1H), 5.71 (d, $^2J_{HH}$ = 14.4 Hz, 1H). ^{13}C NMR (75 MHz, D_2O, δ): 21.9, 21.5 (C(O)*C*H_3), 42.0 (d, $^1J_{PC}$ = 67.1 Hz, P−C−N), 46.7 (d, $^1J_{PC}$ = 64.1 Hz, P−C−N), 53.4 (d, $^1J_{PC}$ = 62.2 Hz, P−C−N), 62.0 (d, $^4J_{PC}$ = 6.86 Hz, N−C−N), 66.9 (d, $^4J_{PC}$ = 6.49 Hz, N−C−N), 169.5 (C(O)), 170.1 (C(O)). ^{31}P NMR (121 MHz, $CDCl_3$, δ): 2.20.

Preparation of Ni(DAPTA)$_4$ (3). To a Schlenk flask containing $Ni(COD)_2$ (0.120 g, 0.436 mmol), in approximately 20 mL of toluene, was added **1** (0.400 g, 1.75 mmol), in 5 mL of methanol, via cannula. The resulting clear solution was stirred for 3 h, leading to the formation of a white precipitate. The white solid was collected by filtration, washed with 2 × 5 mL of ether, and dried under vacuum. Yield: 94.1%. ^1H NMR (300 MHz, CD_2Cl_2, δ): 2.09 (s, 12H, C(O)CH_3), 2.13 (s, 12H, C(O)CH_3), 3.11 (d, $^1J_{HH}$ = 14.4 Hz, 4H, NCHN), 3.48 (s, 8H, PCH_2N), 3.69 (d, $^1J_{HH}$ = 15.3 Hz, 4H, PCHNC(O)), 4.06 (d,

(3) (a) Daigle, D. J.; Peppermann, A. B.; Vail, S. L. *J. Heterocycl. Chem.* **1974**, *11*, 407. (b) Daigle, D. J. *Inorg. Synth.* **1998**, *32*, 40.
(4) (a) Darensbourg, D. J.; Joó, F.; Nádasdi, L.; Bényei, A. Cs. *J. Organomet. Chem.* **1996**, *512*, 45. (b) Smolenski, P.; Pruchnik, F. P. *Appl. Organomet. Chem.* **1999**, *13*, 829.
(5) (a) Darensbourg, D. J.; Joó, F.; Kannisto, M.; Kathó, A.; Reibenspies, J. H.; Daigle, D. J. *Inorg. Chem.* **1994**, *33*, 200. (b) Darensbourg, D. J.; Joó, F.; Kannisto, M.; Kathó, A.; Reibenspies, J. H. *Organometallics* **1992**, *11*, 1990. (c) Darensbourg, D. J.; Stafford, N. W.; Joó, F.; Reibenspies, J. H. *J. Organomet. Chem.* **1995**, *455*, 99.
(6) Daigle, D. J.; Boudreaux, G. J.; Vail, S. L. *J. Chem. Eng. Data* **1976**, *21*, 240.
(7) (a) Darensbourg, D. J.; Yarbrough, J. C.; Lewis, S. J. *Organometallics* **2003**, *22*, 2050.
(8) Hale, G. C. *J. Am. Chem. Soc.* **1925**, *47*, 2754.
(9) (a) Bachmann, W. E.; Horton, W. J.; Jenner, E. L.; MacNaughton, N. W.; Scott, L. B. *J. Am. Chem. Soc.* **1951**, *73*, 2769. (b) Bachmann, W. E.; Deno, N. C. *J. Am. Chem. Soc.* **1951**, *73*, 2777.
(10) (a) Warman, M.; Siele, V. I.; Gilbert, E. E. *J. Heterocycl. Chem.* **1973**, *10*, 97. (b) Siele, V. I.; Warman, M.; Gilbert, E. E. *J. Heterocycl. Chem.* **1974**, *11*, 237.
(11) Siele, V. I. *J. Heterocycl. Chem.* **1977**, *14*, 337.
(12) (a) Grubbs, R. H.; Wang, C.; Friedrich, S.; Younkin, T. R.; Li, R. T.; Bansleben, D. A.; Day, M. W. *Organometallics* **1998**, *17*, 3149. (b) Grubbs, R. H.; Younkin, T. R.; Connor, E. F.; Henderson, J. I.; Friedrich, S.; Bansleben, D. A. *Science* **2000**, *287*, 460.

$^1J_{HH}$ = 13.8 Hz, 4H, PCHNC(O)), 4.28 (d, $^1J_{HH}$ = 15.0 Hz, 4H, NCHN), 4.65 (d, $^1J_{HH}$ = 14.1 Hz, 4H, PCHNC(O)), 4.99 (d, $^1J_{HH}$ = 14.1 Hz, 4H, PCHNC(O)), 5.25 (d, $^1J_{HH}$ = 15.0 Hz, 4H, NCHN), 5.82 (d, $^1J_{HH}$ = 14.4 Hz, 4H, NCHN). ^{13}C NMR (75 MHz, CD_2Cl_2, δ): 21.5 (C(O)*C*H$_3$), 22.2 (C(O)*C*H$_3$), 46.4 (N−C−N), 51.3 (N−C−N), 56.4 (P−C−N), 62.4 (P−*C*−NC(O)), 67.7 (P−*C*−NC(O)), 169.4 (C(O)), 169.8 (C(O)). ^{31}P NMR (121 MHz, CD_2Cl_2, δ): −28.3. IR (CH_2Cl_2): 1643 cm^{-1} (ν(C=O)). Anal. Calcd for $C_{36}H_{64}N_{12}O_8P_4Ni$: C, 44.34; H, 6.56; N, 17.24. Found: C, 44.77; H, 6.57; N, 16.65.

Preparation of Palladium Salicylaldiminato DAPTA Complex (4). To a 50 mL Schlenk flask containing (TMEDA)-Pd(CH_3)$_2$ (150 mg, 0.594 mmol) in 10 mL of toluene at −30 °C was introduced via cannula DAPTA (136 mg, 0.594 mmol) in 5 mL of methanol. To this mixture, the salicylaldimine (208 mg, 0.594 mmol) in 10 mL of toluene at −30 °C was slowly cannulated into the flask, and the solution was stirred for 30 min. The temperature was raised to room temperature, and the light red solution was further stirred overnight. Subsequently, the solvent was removed in vacuo until approximately 5 mL remained, and 20 mL of cold (−78 °C) pentane was added, resulting in the formation of a yellow precipitate. The solid was collected by cold cannula filtration and washed (3 × 5 mL) with cold (−78 °C) pentane, affording **4** in 96.8% yield. ^{1}H NMR (300 MHz, C_6D_6, δ): −0.14 (d, $^3J_{PH}$ = 3.60 Hz, 3H, Pd−CH$_3$), 0.97 (dd, $^3J_{HH}$ = 6.60 Hz, $^3J_{HH}$ = 2.70 Hz, 6H, CH(C*H*$_3$)$_2$), 1.29 (dd, $^3J_{HH}$ = 6.60 Hz, $^3J_{HH}$ = 6.00 Hz, 6H, −C(O)-CH$_3$), 1.80 (d, $^3J_{HH}$ = 6.60 Hz, 6H, CH(C*H*$_3$)$_2$), 2.97−3.02 (m, 1H, DAPTA), 3.24−3.34 (m, 5H, DAPTA), 3.51 (d, $^3J_{HH}$ = 14.10, 1H, DAPTA), 3.62−3.67 (m, 1H, DAPTA), 4.21 (d, $^3J_{HH}$ = 13.80 Hz, 1H, DAPTA), 4.23−4.51 (m, 1H, DAPTA), 6.75 (d, $^3J_{HH}$ = 2.7 Hz, 1H, Ar), 7.11−7.15 (m, 2H, Ar), 7.48 (d, $^3J_{HH}$ = 2.7 Hz, 1H, Ar), 7.55 (d, $^4J_{PH}$ = 11.4 Hz, 1H, HC=N). ^{13}C NMR (75 MHz, C_6H_6, δ): −7.65 (d, $^2J_{PC}$ = 12.2 Hz, Pd−CH$_3$), 21.09, 22.78, 24.56, 28.23, 37.28 (d, $^1J_{PC}$ = 22.05 Hz, P−C−N), 41.97 (d, $^1J_{PC}$ = 19.73 Hz, P−C−N), 47.13 (d, $^1J_{PC}$ = 24.30 Hz, P−C−N), 61.50 (d, $^4J_{PC}$ = 4.50 Hz, C(O)*C*H$_3$), 66.61 (d, $^4J_{PC}$ = 4.50 Hz, C(O)*C*H$_3$), 116.63, 119.75, 123.60, 123.68, 125.53, 127.06, 128.40, 128.74, 129.17, 133.49, 134.44, 140.69 (d, $^3J_{PC}$ = 9.15 Hz, C=N), 146.91, 168.46 (C=O), 169.23 (C=O). ^{31}P NMR (121 MHz, C_6D_6, δ): −24.12. IR (CH_2Cl_2): ν(C=O) = 1605 cm^{-1}. Anal. Calcd for $C_{29}H_{39}N_4O_3PCl_2Pd$: C, 49.79; H, 5.57; N, 8.01. Found: C, 50.06; H, 5.61; N, 7.94.

Preparation of M(CO)$_5$(DAPTA) (M = W (5), Cr (6)) Complexes. The replacement of a single CO molecule was achieved by the photochemical reaction of M(CO)$_6$ in THF. After photolyzing W(CO)$_6$ (0.200 g, 0.57 mmol) in 100 mL of THF, this solution was cannulated over to a flask containing **1** (0.130 g, 0.57 mmol), in 10 mL of THF. The resulting solution was stirred for 1 h followed by removal of the solvent in vacuo. The solid was sublimed to remove any excess W(CO)$_6$. The synthesis of **6** was achieved in an analogous manner. Both complexes are colorless and were cystallized and isolated by the slow evaporation of THF from the corresponding solution, resulting in good yields (>80%). Complexes **5** and **6** are insoluble in water and nonpolar organic solvents (e.g., hexane, pentane), but readily dissolve in polar media (e.g., chloroform, THF).

Complex 5. ^{13}C NMR (75 MHz, CD_2Cl_2, δ): 195.19 (t, dd, $^1J_{WC}$ = 127.75 Hz, $^2J_{PC}$ = 7.16 Hz, CO (*trans*)), 199.07 (d, $^2J_{PC}$ = 21.19 Hz, CO (*eq*)). ^{31}P NMR (121 MHz, CD_2Cl_2, δ): −47.7 (t, $^1J_{WP}$ = 228.52 Hz). Anal. Calcd for $C_{14}H_{16}N_3O_7PW$: C, 30.40; H, 2.92; N, 7.60. Found: C, 30.30; H, 2.94; N, 7.57. IR ($CHCl_3$, cm^{-1}): 1650 ($\nu_{C=O}$, DAPTA), 1944 (E), 2076 (A_1).

Complex 6. ^{31}P NMR (121 MHz, CD_2Cl_2, δ): −5.79. Anal. Calcd for $C_{14}H_{16}N_3O_7PCr$: C, 39.92; H, 3.83; N, 9.97. Found: C, 40.09; H, 3.85; N, 9.98. IR ($CHCl_3$, cm^{-1}): 1658 ($\nu_{C=O}$, DAPTA), 1940 (E).

Water Solubility of 1. The extent of water solubility of **1** was assessed by placing a small, accurately weighed quantity of the ligand in a vial followed by the slow addition of water via a 100 μL syringe with stirring. In a typical experiment, 75 μL of water was needed to completely dissolve 100 mg of **1**. Solubility measurements were repeated several times to yield an average value for the molar solubility of **1** in water of 7.4 M.

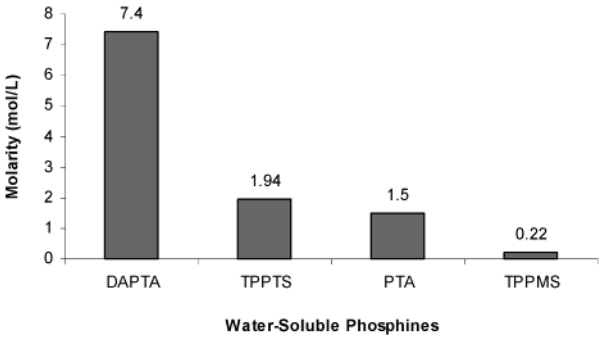

Figure 1. Molar water solubility of selected tertiary water-soluble phosphines.

Results and Discussion

The synthesis of DAPTA and other PTA derivatives was first reported by Siele in 1977.[11] The ligand is easily prepared by direct acylation of PTA in water with acetic anhydride at 0 °C (eq 1).

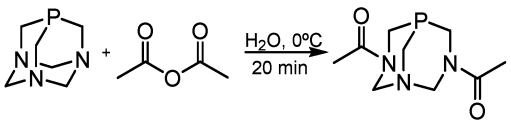

(1)

1

Surprisingly, the water solubility of DAPTA was found to be approximately 7.4 M, making it one of the most water-soluble phosphine ligands thus far reported.[1] A comparison of the water solubility of **1** to its parent, PTA, and the sulfonated triphenylphosphine derivatives (i.e., TPPMS and TPPTS)[13] illustrates its superior water solubility characteristic (Figure 1). Additionally, the ligand readily dissolves in common organic solvents such as methylene chloride, acetone, and alcohols (e.g., methanol and ethanol), making it a very versatile ligand that may be used in a variety of solvents.

The previously reported NMR data for **1** by Siele were obtained on a 60 MHz instrument, and therefore, no detailed splitting patterns or coupling constants were provided. Here, we wish to point out some of these key features by examining the ^{1}H, ^{13}C, and ^{31}P spectra of the phosphine. All of the ^{1}H NMR resonances associated with the methylene carbons exhibit phosphorus coupling ($^xJ_{PH}$, x = 2, 4) on the order of 13 Hz. The methyl hydrogens on the acyl functionality (C(O)C*H*$_3$) are observed as a singlet at 1.96 ppm. In the ^{13}C NMR spectrum in $CDCl_3$, the acyl carbons N*C*(O)CH$_3$ are displayed by a single resonance at 168.96 ppm, which is contrary to what is expected for the *anti* conformation (vide infra). On the other hand, both the ^{13}C and ^{1}H NMR spectra of **1** indicate a mixture of conformers present in aqueous solution. For example, the ^{13}C NMR resonances (N*C*(O)CH$_3$) occur at 172.2 and 171.7 ppm,

(13) (a) Kuntz, E. G. *CHEMTECH* **1987**, *17*, 570. (b) Kuntz, E. G. French Patent 2314910, 20.06, 1975. (c) Kuntz, E. G. US Patent Re 31812, 29.05, 1982.

Table 1. Crystallographic Data for Complexes 1, 2, 4, 5, and 6

	1	2	4	5	6
cryst syst	monoclinic	orthorhombic	triclinic	monoclinic	orthorhombic
space group	*P*2(1)	*Pbca*	$P\bar{1}$	*P*2(1)/*c*	*Pbca*
V, Å^3	535.3(11)	2224(4)	3350.3(16)	1843.8(7)	3633(7)
Z	2	8	4	4	8
a, Å	6.191(7)	8.506(10)	12.530(4)	12.000(2)	11.836(13)
b, Å	10.431(12)	11.121(13)	15.620(4)	12.922(3)	13.693(14)
c, Å	8.407(10)	23.51(3)	17.576(5)	13.238(3)	22.41(2)
α, deg			77.533(5)		
β, deg	99.59(2)		85.937(5)	116.076(4)	
γ, deg			88.832(5)		
T, K	110	110	110	110	110
d(calc), g/cm^3	1.422	1.465	1.570	1.993	1.541
abs coeff, mm^{-1}	0.242	0.245	0.960	6.393	0.759
R,[a] % [$I > 2\sigma(I)$]	10.59	6.17	7.93	5.26	3.09
R_w,[a] %	19.23	6.86	10.24	6.49	4.66

[a] $R = \sum||F_o| - |F_c||/\sum F_o$ and $R_{wF} = \{[\sum w(F_o - F_c)^2]/\sum wF_o^2\}^{1/2}$.

Scheme 1

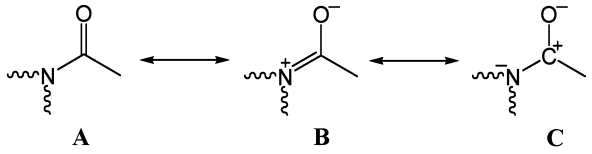

with the latter being about one-fourth the intensity of the former. The two acyl groups adopt an *anti* conformation in the solid state (vide infra), with the barrier to rotation of the N−C(O) bond generally ascribed to the π electronic resonance model of an amide (**A** and **B** in Scheme 1).[14a] This experimental rotational barrier is expected to be about 18−19 kcal/mol.[14b−d] More recent ab initio computations assign a large part of the rotational stability of the N−C bond to a Coulombic interaction via the σ system between the N and carbonyl C atoms (**C** in Scheme 1).[14e] Further upfield are the resonances pertaining to the P−C−N carbons, which fall at 67.0 and 70.1 ppm, respectively. Those associated with the N−C−N carbons are found at 62.0 ppm.

Dissolving **1** in CH_2Cl_2 and allowing the slow diffusion of pentane into the solution over several days at −20 °C resulted in quality crystals for X-ray diffraction. The crystallographic data and selected bond distances and angles are presented in Table 1 and Table 2, respectively. A thermal ellipsoid representation of **1** is shown in Figure 2. In the solid state, the $C(O)CH_3$ groups are *anti* with respect to each other. The N(2)−C(6) and N(3)−C(7) bond distances were found to be short when compared to other N−C bond distances, with values of 1.373(18) and 1.377(18) Å, respectively, and resemble a Schiff base (N=C) double bond (Scheme 1). The P(1)−C(1) bond distance was found to be approximately 0.03 Å longer than the P(1)−C(2) counterpart, but is nevertheless significantly shorter than that found in the P−C bond lengths of PTA (i.e., 1.857(3) Å).[15]

Table 2. Selected Bond Distances (Å) and Angles (deg) for Compounds 1, 2, 4, 5, and 6[a]

Compound 1			
P(1)−C(1)	1.736(15)	C(6)−C(8)	1.524(19)
P(1)−C(2)	1.707(14)	N(3)−C(7)	1.377(18)
P(1)−C(3)	1.742(14)	C(7)−O(2)	1.258(14)
N(2)−C(6)	1.373(18)	C(7)−C(9)	1.483(19)
C(6)−O(1)	1.224(15)		
P(1)−C(1)−N(2)	118.5(9)	C(1)−N(2)−C(6)	116.0(10)
P(1)−C(2)−N(3)	119.9(10)	C(2)−N(3)−C(7)	124.7(11)
P(1)−C(3)−N(1)	115.0(10)		
Compound 2			
P(1)−C(1)	1.816(3)	C(6)−O(1)	1.227(4)
P(1)−C(2)	1.827(3)	C(6)−C(8)	1.500(5)
P(1)−C(3)	1.797(3)	N(3)−C(7)	1.360(4)
P(1)−O(3)	1.492(3)	C(7)−O(2)	1.236(4)
N(2)−C(6)	1.365(4)	C(7)−C(9)	1.499(4)
P(1)−C(1)−N(2)	111.80(18)	C(1)−N(2)−C(6)	118.5(2)
P(1)−C(2)−N(3)	114.57(19)	C(2)−N(3)−C(7)	123.3(2)
P(1)−C(3)−N(1)	106.19(18)		
Complex 4			
Pd(1)−C(1)	2.029(8)	Pd(1)−P(1)	2.209(2)
Pd(1)−N(1)	2.080(6)	Pd(1)−O(1)	2.077(5)
C(1)−Pd(1)−O(1)	175.4(3)	P(1)−Pd(1)−O(1)	86.91(16)
P(1)−Pd(1)−C(1)	88.5(3)	P(1)−Pd(1)−N(1)	177.82(17)
O(1)−Pd(1)−N(1)	90.9(2)		
Compound 5			
P(1)−C(1)	1.840(11)	W(1)−C(11)	2.053(13)
P(1)−C(2)	1.849(10)	W(1)−C(12)	1.999(13)
P(1)−C(3)	1.845(11)	N(3)−C(7)	1.348(13)
W(1)−P(1)	2.492(3)	C(7)−O(2)	1.230(12)
W(1)−C(10)	2.049(14)	C(7)−C(9)	1.519(15)
N(2)−C(6)	1.344(13)	W(1)−C(13)	2.032(13)
C(6)−O(1)	1.224(13)	W(1)−C(14)	2.040(13)
C(6)−C(8)	1.535(15)		
P(1)−C(1)−N(2)	117.6(7)	C(1)−N(2)−C(6)	119.1(9)
P(1)−C(2)−N(3)	112.4(7)	C(2)−N(3)−C(7)	124.5(9)
P(1)−C(3)−N(1)	109.8(7)	C(10)−W(1)−P(1)	176.1(3)
C(11)−W(1)−P(1)	90.0(3)	C(10)−W(1)−C(11)	88.3(4)
C(12)−W(1)−P(1)	92.7(4)	C(10)−W(1)−C(12)	90.8(5)
Compound 6			
P(1)−C(1)	1.853(3)	Cr(1)−C(11)	1.910(4)
P(1)−C(2)	1.839(3)	Cr(1)−C(12)	1.902(4)
P(1)−C(3)	1.836(3)	N(3)−C(7)	1.359(4)
Cr(1)−P(1)	2.3562(19)	C(7)−O(2)	1.227(4)
Cr(1)−C(10)	1.863(4)	C(7)−C(9)	1.512(5)
N(2)−C(6)	1.359(4)	Cr(1)−C(13)	1.902(4)
C(6)−O(1)	1.233(4)	Cr(1)−C(14)	1.903(4)
C(6)−C(8)	1.504(5)		
P(1)−C(1)−N(2)	113.8(2)	C(1)−N(2)−C(6)	124.7(3)
P(1)−C(2)−N(3)	114.93(19)	C(2)−N(3)−C(7)	118.2(2)
P(1)−C(3)−N(1)	109.9(2)	C(10)−Cr(1)−P(1)	173.55(10)
C(11)−Cr(1)−P(1)	89.31(12)	C(10)−Cr(1)−C(11)	87.37(15)
C(12)−Cr(1)−P(1)	94.56(11)	C(10)−Cr(1)−C(12)	91.00(14)

[a] Estimated standard deviations are given in parentheses.

As evident from the space-filling model, the rigid nature of the ligand creates a cavity within the cage structure (Figure 3). The phosphorus atom is clearly exposed, allowing for easy binding to a metal center. Additionally, the acyl-free nitrogen and oxygen atoms are also exposed, which facilitates hydrogen bonding to the surrounding aqueous environment. The calculated cone angle was found to be similar to that reported for PTA, having a value of about 102°.[16]

The phosphine oxide species **2** was also fully characterized in solution and in the solid state. This derivative

(14) (a) Yamada, S. *J. Org. Chem.* **1996**, *61*, 941. (b) Sunner, B.; Piette, L. H.; Schneider, W. G. *Can. J. Chem.* **1960**, *38*, 681. (c) Kamei, H. *Bull. Chem. Soc. Jpn.* **1968**, *41*, 2269. (d) Drakenberg, T.; Forsen, S. *J. Phys Chem.* **1970**, *74*, 1. (e) Wiberg, K. B.; Breneman, C. M. *J. Am. Chem. Soc.* **1992**, *114*, 831.

(15) Fluck, E.; Förster, J.; Weidlein, J.; Hidiche, E. *Z. Naturforsh.* **1977**, *32b*, 409.

(16) Delerno, J. R.; Trefonas, L. M.; Darensbourg, M. Y.; Majeste, R. J. *Inorg. Chem.* **1976**, *15*, 816.

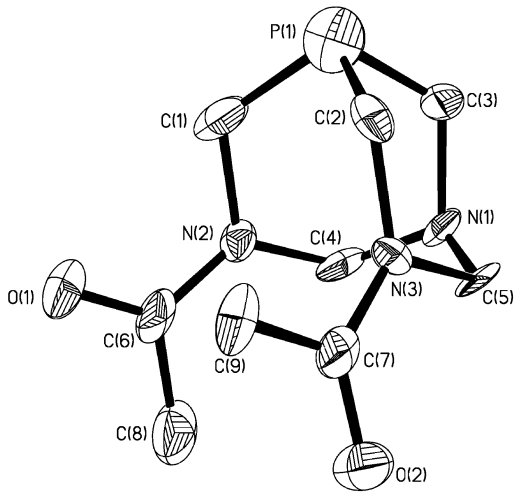

Figure 2. Thermal ellipsoid representation of DAPTA (**1**) showing 50% probability ellipsoids.

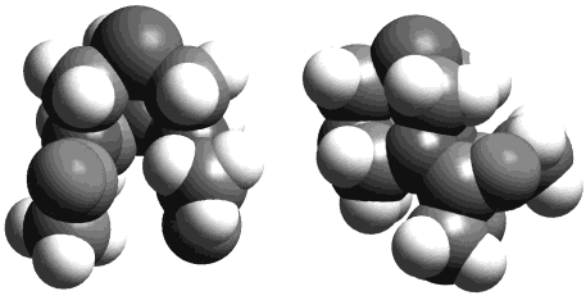

Figure 3. Space-filling model of DAPTA (**1**) showing (a) front and (b) side view.

is easily prepared from PTA oxide employing the same synthetic strategy used in the synthesis of **1** (eq 2).

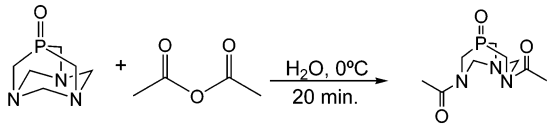

(2)

2

Spectroscopically, **2** is similar to its parent. Although difficult to interpret, the ^{1}H NMR spectrum displays coupling between geminal hydrogens. For example, the proton (H_A) associated with the N−CH−N framework and in the axial position is shielded more by the *syn* C═O group residing on the adjacent nitrogen and therefore is located further downfield at 5.71 ppm. Meanwhile, its geminal hydrogen, residing in the equatorial position, is less shielded and appears further upfield with a common $^{2}J_{HH}$ coupling constant (i.e., 14.4 Hz) (Figure 4). ^{31}P coupling is observed for the P−CH_2−N protons, located at 3.27 ppm, and is on the order of 6.60 Hz. Similar to **1**, the ^{13}C NMR spectrum is also easy to interpret and displays several signals with ^{31}P coupling. For example, the P−C−N carbons are located at 41.99, 46.72, and 53.40 ppm with $^{1}J_{PC}$ constants of 62−67 Hz. The coupling between these hydrogens and phosphorus illustrates the pronounced electronic effect of oxygen. The two C═O signals reside at 169.45 and 170.09 ppm with an absence of ^{31}P coupling.

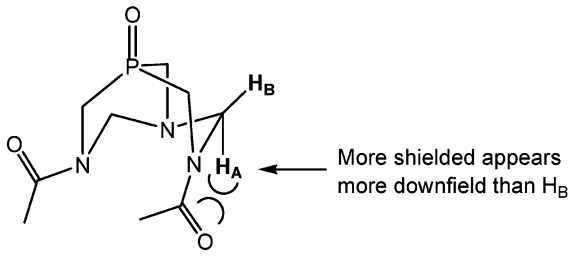

Figure 4. Shielding effects on geminal protons by acyl group in DAPTA oxide (**2**).

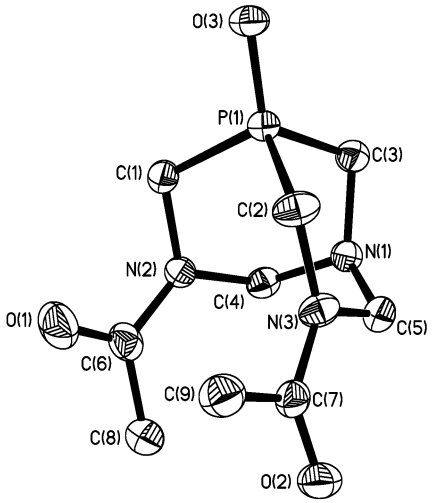

Figure 5. Thermal ellipsoid representation of DAPTA oxide (**2**) showing 50% probability ellipsoids.

Allowing a concentrated CH_2Cl_2 solution of **2** to stand at −20° C over a period of two weeks resulted in the formation of large, colorless, single crystals. Using these crystals for X-ray analysis, a solid state structure of **2** was obtained. Crystallographic data and selected bond distances and angles are provided in Tables 1 and 2, respectively. A thermal ellipsoid representation of **2** is shown in Figure 5. A key feature in the solid state, as was also observed in complexes **5** and **6**, is the P(1)−C(Y) (Y = 1−3) bond distances. Upon coordination of the ligand to a metal or in its oxidized form, these bond lengths are approximately 0.09 Å longer than those observed in **1**. However, the N(2)−C(6) and N(3)−C(7) are nearly identical when compared to its parent, as is the case for many of the other bond distances. The P(1)−O(3) bond distance is found to have a value of 1.492(3) Å. In the space-filling model, the ligand also possesses the cavity observed in **1** with the oxygen atom coordinated to phosphorus fully exposed for binding (Figure 6). The other oxygen atoms as well as the acyl-free nitrogen is also exposed, similar to **1**.

Several complexes incorporating **1** were synthesized to illustrate the binding mode and strength of this phosphine. PTA complexes of group 10 metals have been previously reported and were found to be readily soluble in water. Of main interest is the nickel(0) PTA complex, $Ni(PTA)_4$, which can be synthesized from $Ni(COD)_2$ and 4 equiv of PTA in a toluene/methanol solution. Using

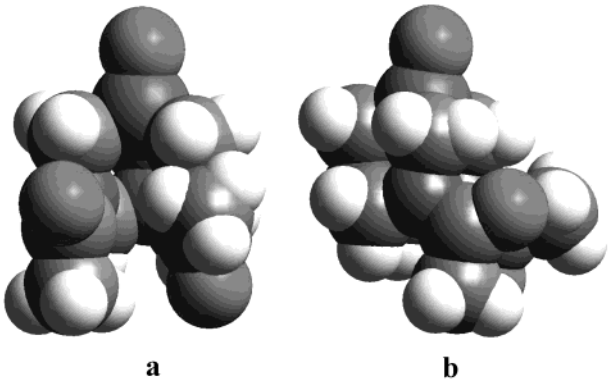

Figure 6. Space-filling model of DAPTA oxide (**2**) showing (a) front and (b) side view.

Scheme 2

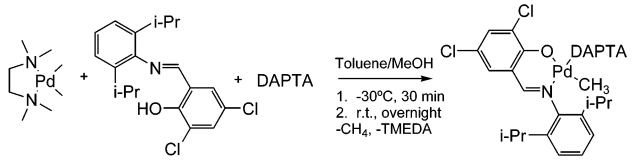

this methodology, the Ni(DAPTA)$_4$ (**3**) derivative was prepared (eq 3).

$$\mathrm{Ni(COD)_2} + 4\ \mathrm{DAPTA} \xrightarrow[2\ \mathrm{h,\ rt}]{\mathrm{toluene/methanol}} \underset{\mathbf{3}}{\mathrm{Ni(DAPTA)_4}} + 2\ \mathrm{COD} \quad (3)$$

The product was characterized by ^{1}H, ^{13}C, and ^{31}P NMR as well as elemental analysis. Unfortunately, **3** is not soluble in water or alcoholic solvents such as methanol or ethanol, but is readily soluble in chlorinated organic solvents such as methylene chloride. The insoluble nature of the complex in water is surprising due to the high water solubility of **1** and Ni(PTA)$_4$ (0.291 M).[17] The IR spectrum displays the ν(C═O) stretch at 1643 cm^{-1}, which is nearly identical to the ν(C═O) stretch of the free ligand in CH_2Cl_2. The ^{13}C NMR spectrum displays the two signals due to the acyl carbons at 169.8 and 169.4 ppm, respectively, while the ^{1}H NMR contains many signals that are split by phosphorus and geminal coupling. Attempts to grow suitable crystals in CH_2Cl_2 have failed due to the formation of spherical crystals, all of which did not diffract upon exposure to X-ray radiation.

Another group 10 metal complex bearing **1** is the salicylaldiminato palladium complex **4**. This derivative was prepared using the synthetic methodology employed for the synthesis of palladium salicylaldiminato PTA complexes (Scheme 2).[18] In solution, the complex is very similar to its PTA analogue. For example, the ketimine hydrogen, HC═N, exhibits $^4J_{PH}$ coupling on the order of 11.4 Hz, which is slightly larger than that reported for the PTA analogue (i.e., 10.5 Hz). The isopropyl groups on the aniline moiety are perpendicular to the plane and exhibit a rotation barrier, as two sets of signals are observed in the ^{1}H NMR spectrum for the

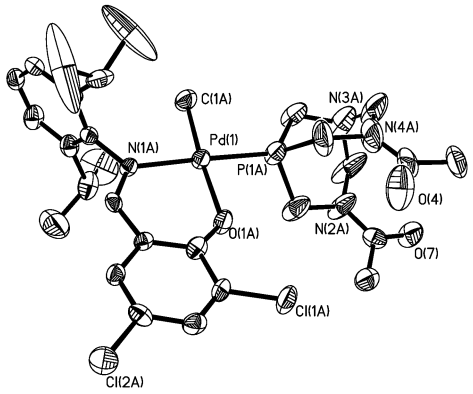

Figure 7. Thermal ellipsoid representation of **4** showing 50% probability ellipsoids.

CH(C*H*$_3$)$_2$ hydrogens. The ν(C═O) stretch was found to be located at 1605 cm^{-1}, which is approximately a 50 cm^{-1} shift to lower frequency from that of the free ligand. Additionally, a rotation barrier exists about the N−C(O)CH$_3$ bonds, as two sets of signals are observed in the ^{13}C NMR spectrum for the *C*(O)CH$_3$ groups.

Allowing the slow diffusion of pentane into a toluene solution of **4** at −20 °C resulted in X-ray quality crystals. Crystallographic data and selected bond distances and angles are shown in Tables 1 and 2, respectively. A thermal ellipsoid representation of **4** is presented in Figure 7. The solid state structure of the complex is nearly identical to its PTA analogue, with the Pd(1)−P(1) bond distances being the same in both complexes (i.e., 2.209(2) and 2.211(3) Å for **4** and the PTA analogue, respectively).[18] The palladium metal center adopts the standard square-planar geometry, as the C(1)−Pd(1)−O(1) and P(1)−Pd(1)−N(1) bond angles are found to have values of 175.4(3)° and 177.82(17)°, respectively.

Group 6 pentacarbonyl complexes of DAPTA were also prepared by the typical reaction protocol of photolyzing a THF solution of M(CO)$_6$ (M = W, Cr) to produce the M(CO)$_5$(THF) intermediate. Following the in situ formation of M(CO)$_5$(THF), a THF solution of **1** was added, yielding the M(CO)$_5$(DAPTA) (M = W (**5**), Cr (**6**)) complexes in good yields (eq 4). For the tungsten

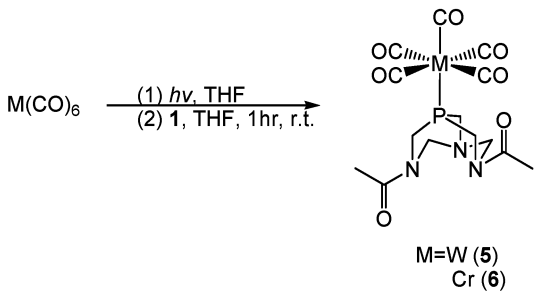

(4)

derivative, **5**, the ν(C═O) stretch associated with bound **1** was found to be located at 1663 cm^{-1} in THF, a 10 cm^{-1} shift to higher energy when compared to the free ligand. In the 195−200 ppm region of the ^{13}C NMR, the two signals pertaining to the M−*C*O carbons are observed with pronounced ^{31}P and ^{183}W coupling. The signal at 195.2 ppm, due to the equatorial carbonyls, has a $^1J_{WC}$ and $^2J_{PC}$ coupling of 127.8 and 7.3 Hz, respectively. The resonance at 199.1 ppm, derived from the axial carbonyl, exhibits a ^{31}P coupling of 21.2 Hz with no visible ^{183}W coupling due to the lower signal

(17) Darensbourg, D. J.; Decuir, T. J.; Stafford, N. W.; Robertson, J. B.; Draper, J. D.; Reibenspies, J. H.; Kathó, A.; Joó, F. *Inorg. Chem.* **1997**, *36*, 4218.

(18) Darensbourg, D. J.; Ortiz, C. G.; Yarbrough, J. C. *Inorg. Chem.* **2003**, *42*, 6915.

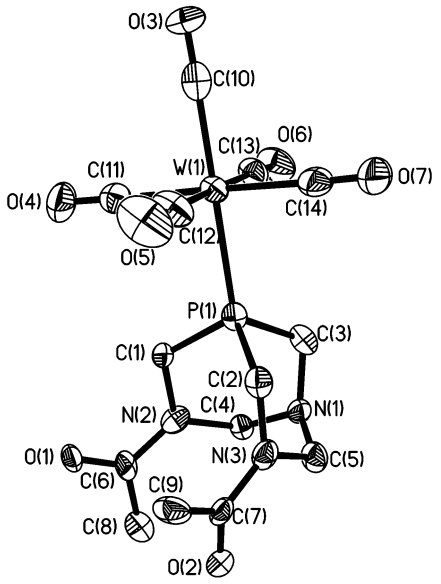

Figure 8. Thermal ellipsoid representation of $W(CO)_5$(DAPTA) (**5**) showing 50% probability ellipsoids.

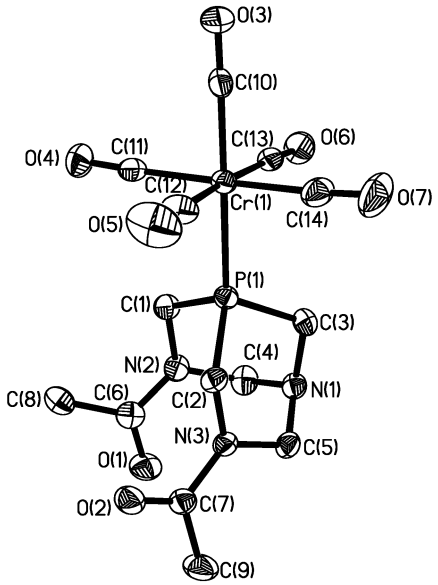

Figure 9. Thermal ellipsoid representation of $Cr(CO)_5$(DAPTA) (**6**) showing 50% probability ellipsoids.

intensity. The ^{31}P resonance is located at −47.7 ppm, an approximate 25 ppm upfield shift from the free ligand, with $^1J_{WP}$ coupling of 228.5 Hz, which is similar to that observed for the $W(CO)_5$(PTA) ($^1J_{WP}$ = 218.2 Hz) and $W(CO)_5(PASO_2)$ ($^1J_{WP}$ = 228.9 Hz) complexes.[7]

Colorless crystals suitable for X-ray diffraction were isolated by the slow evaporation of THF from a corresponding solution of the complex at room temperature. Crystallographic data and selected bond distances and angles for the complex are presented in Tables 1 and 2, respectively. A thermal ellipsoid representation of the complex showing 50% probability is shown in Figure 8. The tungsten metal center exhibits a slightly distorted octahedral coordination, with the C(12)−W(1)−C(13), C(10)−W(1)−P(1), and C(11)−W(1)−C(14) bond angles having values of 179.7(5)°, 176.1(3)°, and 177.3(5)°, respectively. The pronounced shorter $W-C_{ax}$ bond distance observed for the axial carbonyl in the $W(CO)_5$(PTA) and $W(CO)_5(PASO_2)$ complexes is not observed in **5**.[7] All W−C bond distances have an average value of 2.044 Å. The W(1)−P(1) bond distance is very similar to the PTA analogue, with a value of 2.492(3) Å, and is shorter than the W−P distance of 2.516 Å of the trimethylphosphine analogue, $W(CO)_5(PMe_3)$.[19a]

Using the same crystal growth technique, crystals of **6** suitable for X-ray analysis were obtained. Crystallographic data and selected bond distances and angles are presented in Tables 1 and 2, respectively. A thermal ellipsoid representation showing 50% probability of the complex is provided in Figure 9. The chromium metal center exhibits a slightly distorted octahedral geometry, with the C(12)−Cr(1)−C(13), C(10)−Cr(1)−P(1), and C(11)−Cr(1)−C(14) bond angles having values of 175.55(14)°, 173.55(10)°, and 177.30(14)°, respectively. Although not observed in **5**, the axial Cr(1)−C(10) distance is appreciably shorter than the equatorial Cr−CO, with a value of 1.863(4) Å. This is approximately 0.04 Å shorter than the average Cr−C bond distance pertaining to the equatorial carbonyls. The Cr(1)−P(1) bond distance was found to be 2.3562(19) Å, which is approximately 0.01 Å shorter than that found in the $Cr(CO)_5PMe_3$ analogue.[19b,c] Furthermore, the pronounced tilt associated with the phosphine ligand and the equatorial carbonyl plane observed for the PTA and $PASO_2$ tungsten pentacarbonyl derivatives is not present in complexes **5** and **6**.[7]

Concluding Remarks

The cage-opening reaction of PTA and its oxide with acetic anhydride to provide the corresponding acylated products **1** and **2**, respectively, has been revisited. In this report we have fully characterized these derivatives in solution by $^1H/^{13}C/^{31}P$ NMR and infrared spectroscopies, as well as in the solid state by X-ray crystallography. As anticipated, restricted rotation about the amide nitrogen−carbonyl carbon bond is observed, which is consistent with the short N−C(O) bond distances determined in these derivatives. Phosphine **1** was shown to possess excellent solubility in water (7.4 M), much greater than that of its PTA analogue. In accordance with the water solubility of **1**, its $\nu_{C=O}$ vibration in water occurs at 1608 cm^{-1}, some 34 cm^{-1} to lower energy than that observed in weakly interacting organic solvents. This is indicative of a strong interaction of the amide nitrogen−CO bond dipole with water.

The binding ability of DAPTA (**1**) toward a variety of metal centers was shown to be very much comparable to that of the parent PTA ligand, which in turn compares favorably with the air-sensitive PMe_3 ligand. This is evident in the M−P bond distances observed in corresponding metal complexes of **1** and PTA. For example, the W−P bond distances in $(CO)_5$W(PTA), $(CO)_5$W(DAPTA), and $(CO)_5WPMe_3$ are 2.4976(15), 2.492(3), and 2.516(3) Å, respectively. Further evidence for the relative binding abilities of **1** and PTA was provided by the similarities in the ν(CO) vibrational modes in $M(CO)_5L$ derivatives, where M = Cr or W and L = **1** or

(19) (a) Cotton, F. A.; Darensbourg, D. J.; Kolthammer, B. W. S. *Inorg Chem*. **1981**, *20*, 4440. (b) Davies, M. S.; Pierens, R. K.; Aroney, M. J. *J. Organomet. Chem*. **1993**, *458*, 141. (c) Lee, K. J.; Brown, T. L. *Inorg. Chem*. **1992**, *31*, 289.

PTA.[20] Unexpectedly, the $Ni(DAPTA)_4$ (**3**) derivative, which is highly soluble in organic solvents, exhibits no solubility in water, whereas its $Ni(PTA)_4$ analogue is very water soluble. We will continue our efforts to obtain X-ray quality crystals of this derivative in hopes that its solid state structure will shed some light on this puzzling issue. Finally, it should be possible to synthesize other phosphine ligands via this cage-opening reaction, which possess a wide range of solubility and metal-binding properties.[21,22]

(20) Darensbourg, M. Y.; Daigle, D. J. *Inorg. Chem*. **1975**, *14*, 1217.
(21) An alternative cage-opened PTA derivative which serves as a chelating ligand has been reported by Schmidbaur and co-workers.[22]
(22) Assmann, B.; Angermaier, K.; Paul, M.; Riede, J.; Schmidbaur, H. *Chem. Ber*. **1995**, *128*, 891.

Acknowledgment. Financial support from the National Science Foundation (CHE 02-34860 and CHE 98-07975 for purchase of X-ray equipment) and the Robert A. Welch Foundation is greatly appreciated.

Note Added after ASAP. In the version of the paper originally posted on the web on March 9, 2004, Figures 5 and 6 were incorrectly repeated as Figures 2 and 3. The version that now appears is correct.

Supporting Information Available: Complete details of the X-ray diffraction studies on compounds **1**, **2**, and **4**-**6**. This material is available free of charge via the Internet at http://pubs.acs.org.

OM0343059